https://doi.org/10.5194/egusphere-2026-5887
Preprint. Discussion started: 9 November 2026
© Author(s) 2026. CC BY 4.0 License.

Decoupling chemical formation and vertical recirculation in driving urban ozone pollution

Zhenguo Liu[1], Yu Zou[2,*], Xin Song[1], Xiao-Bing Li[1,*], Bin Yuan[1], Chenglei Pei[3], Yuwen Peng[3], Jing Chen[1], Xuemei Wang[1], Min Shao[1]

[1] College of Environment and Climate, Institute for Environmental and Climate Research, Guangdong-Hongkong-Macau Joint Laboratory of Collaborative Innovation for Environmental Quality, Jinan University, Guangzhou 511443, China

[2] Guangzhou Institute of Tropical and Marine Meteorology of China Meteorological Administration, GBA Academy of Meteorological Research, Guangzhou, 510640, China

[3] Guangzhou Sub-branch of Guangdong Ecological and Environmental Monitoring Center, Guangzhou, 510006, China

[*] Corresponding authors: Yu Zou (yzou@gd121.cn) and Xiao-Bing Li (lixiaobing@jnu.edu.cn)

https://doi.org/10.5194/egusphere-2026-5887
Preprint. Discussion started: 9 November 2026
© Author(s) 2026. CC BY 4.0 License.



Abstract

Surface ozone pollution in subtropical urban regions exhibits strong seasonal differences in its driving mechanisms, but it is still unclear at present. Here, based on integrated ground-based and vertical measurements of ozone and its precursors in the Pearl River Delta region, this study finds that ozone exceedances in the wet season are primarily driven by intense local photochemistry, linked to higher temperatures and biogenic emissions. In contrast, the observed dry-season period pollution episodes are dominated by the downward entrainment of ozone within the planetary boundary layer (PBL), where the stored ozone in aloft is transported downward as the PBL expands. During these events, downward transport (including regional transport) contributes 58%–90% of the boundary-layer ozone enhancement (08:00–14:00 LT), whereas local photochemistry plays a minor role (3%–31%). These results imply that short-term emission controls are less effective in the dry season. Proactive reduction of precursors ahead of stable weather conditions may therefore help alleviate the buildup of ozone in the high atmosphere.

Keywords: Volatile organic compounds; Ozone pollution; Photochemistry; Downward entrainment

https://doi.org/10.5194/egusphere-2026-5887
Preprint. Discussion started: 9 November 2026
© Author(s) 2026. CC BY 4.0 License.

1. Introduction

Surface ozone (O_3), a typical photochemical pollutant, has become a key factor affecting urban air quality worldwide *(Agathokleous et al., 2023; Li et al., 2021a; Perdigones et al., 2022; He et al., 2020)*. The Pearl River Delta (PRD) region is a subtropical coastal megalopolis and has achieved remarkable reductions in fine particulate matter ($PM_{2.5}$) concentrations *(Shao et al., 2021)*. However, ozone pollution has emerged as a growing concern *(Li et al., 2022a)*, now standing as the principal pollutant hindering the further improvement of regional air quality. Unlike in temperate zones where ozone usually peaks in summer *(He et al., 2008)*, the PRD exhibits a distinct seasonal pattern *(Li et al., 2022a)*. Ozone pollution generally occurs in both the dry season (typically autumn and winter) and the wet season (spring and summer) *(Li et al., 2012)*, with notable wintertime ozone episodes reported in recent years *(Song et al., 2024; Li et al., 2021a)*. A deep understanding of the physico-chemical processes underlying these seasonal differences is a scientific prerequisite for designing precise and effective ozone control strategies.

The formation mechanisms of ozone pollution are complex, as ambient ozone concentrations result from the nonlinear interplay of multiple factors *(Cheng et al., 2018; Wang et al., 2017)*. These include emissions of precursors (namely nitrogen oxides (NOx) and volatile organic compounds (VOCs)), meteorological conditions, vertical and horizontal transport *(Zhang et al., 2022)*. Key challenges and ongoing debates in current research include the following aspects. First, the ozone-precursor relationship is highly nonlinear. The effects of emission reduction strategies are highly dependent on the chemical formation regime of ozone (e.g., whether it is VOCs-limited or NOx-limited) *(Perdigones et al., 2022; Yang et al., 2021; Zhao et al., 2022)*. Second, the relative contributions of natural (e.g., biogenic VOCs emissions) versus anthropogenic sources to ozone production remain uncertain *(Wang et al., 2022b; Wang et al., 2022a; Cao et al., 2022; Pfannerstill et al., 2024; Qin et al., 2025)*. More critically, the relative contributions of local photochemical production and vertical transport to the budgets of surface ozone is hardly to be quantified *(Wu et al., 2023; Yates et al., 2015; Mathur et al., 2018; Udina et al., 2020; Zhou et al., 2025; Ma et al., 2025)*, particularly in urban regions with strong and complex precursor emissions *(Song et al., 2024)*.

Previous studies indicate significant vertical variations in both the formation

https://doi.org/10.5194/egusphere-2026-5887
Preprint. Discussion started: 9 November 2026
© Author(s) 2026. CC BY 4.0 License.

mechanisms and production efficiency of ozone in the planetary boundary layer (PBL) *(Li et al., 2025; Wang et al., 2025; Li et al., 2024; Xing et al., 2024)*, with generally higher concentrations aloft *(Ding et al., 2008; Li et al., 2017)*. The subsequent downward entrainment of ozone via daytime PBL mixing is recognized as an important contributor to surface ozone buildup *(Li et al., 2021b; Klein et al., 2019)*. Quantifying the contribution of this vertical transport to the enhancement of surface ozone is therefore essential. However, for subtropical regions like the PRD, which is influenced by unique monsoon circulation and complex synoptic systems (e.g., the subtropical high and typhoons) *(Huang et al., 2006)*, the seasonal variation and relative importance of these processes between dry and wet seasons remain poorly understood.

In PRD, distinctly different meteorological and boundary-layer structures between wet and dry seasons drive a shift in the dominant ozone formation mechanisms. The dry season is typically governed by continental high-pressure systems or weak cold high-pressure ridges *(Huang et al., 2005)*. Conditions are characterized by clear skies, low humidity and temperature, strong solar radiation and atmospheric stability, all favoring efficient local photochemistry. Moreover, the strong atmospheric stability suppresses the vertical dilution of pollutants, potentially aiding the preservation of ozone aloft and its subsequent downward transport *(Song et al., 2024)*. In contrast, the wet season features high temperatures and humidity. Frequent precipitation also provides a scavenging effect on air pollutants, contributing to generally lower mean ozone concentrations compared to the dry season *(Li et al., 2022a)*. However, the warmer temperatures in wet season largely enhance emissions of highly reactive VOCs from biogenic sources *(Pfannerstill et al., 2024; Song et al., 2025; Zeng et al., 2023)*, potentially accelerating local photochemical ozone formation *(Wang et al., 2022b; Canaval et al., 2020)*. Furthermore, previous studies have noted that the ozone pollution episodes in wet season are often associated with specific synoptic patterns, particularly the peripheral circulation of typhoons *(Wang et al., 2022b; Huang et al., 2006)*. Subsidence motions of air parcels at the periphery of a typhoon can effectively transport ozone from the free troposphere into the PBL *(Lu et al., 2026)*, significantly elevating surface ozone concentrations. Therefore, clarifying the relative importance of local photochemical formation versus vertical transport in driving ozone pollution during the dry and wet seasons is fundamental to a deeper understanding of ozone pollution formation in the PRD.

https://doi.org/10.5194/egusphere-2026-5887
Preprint. Discussion started: 9 November 2026
© Author(s) 2026. CC BY 4.0 License.

In this study, we quantify the roles of local photochemical production and vertical transport in driving surface ozone pollution across different seasons in the PRD. The analysis utilizes one year of observational data from an urban monitoring site, including ozone, NOx, VOCs, and meteorological parameters. This dataset is further enhanced by vertical gradient measurements of ozone and nitrogen dioxide (NO_2) from the surface to 488 m on the Canton Tower. Using these observational constraints, box model simulations were conducted to quantify ozone formation and removal pathways, assess its formation sensitivity to precursors, and estimate production rates. The findings are intended to provide scientific support for formulating effective ozone control strategies in the PRD. We also anticipate that this work will offer useful insights for other subtropical monsoon-affected cities facing similar challenges with seasonal ozone pollution.

2. Methods

2.1 Data acquisition

Measurements of air pollutants and meteorological factors were conducted in Panyu District, Guangzhou in the PRD, from July 1, 2024, to June 30, 2025 (Fig. 2). Hourly concentrations of air pollutants, including O_3, NO, NO_2, $PM_{2.5}$, PM_{10}, SO_2, and CO, were collected from a national environmental monitoring station located at Guangzhou Panyu Middle School (GPMS, located at 22°56'N, 113°21'E). Hourly meteorological data, such as wind speed, wind direction, atmospheric pressure (P), temperature (T), and relative humidity (RH), were obtained from a nearby National Basic Meteorological Station (22°57'N, 113°22'E). The configurations of the instruments used for measuring air pollutants and meteorological parameters are described in SI and are consistent with those reported in previous studies *(Li et al., 2022a; Zou et al., 2015)*.

Continuous measurements of VOCs were conducted over a one-year period at the Guangzhou Panyu Atmospheric Composition Station (GPACS, located at 23°00'N, 113°21'E). The station is situated on a mountaintop at an elevation of 141 m. Surrounded by residential areas with no major industrial emission sources nearby, this location is representative of a typical urban environment in the PRD *(Zou et al., 2015)*. The determination of VOCs components (NMHCs + OVOCs) in ambient air in Guangzhou was performed using an online GC-MS/FID instrument (Model TH-300B,

https://doi.org/10.5194/egusphere-2026-5887
Preprint. Discussion started: 9 November 2026
© Author(s) 2026. CC BY 4.0 License.

Wuhan Tianhong Environmental Protection Industry Co., Ltd.). The system features two separate gas pathways. The FID channel is used to detect C2–C5 compounds, while the MS detection channel is used to detect C5–C12 compounds, covering a total of 116 VOCs. Instrument principles and operational procedures are described in the literature *(Zou et al., 2025; Zou et al., 2024)* and are not repeated here. As illustrated in Fig. S1, the distances from this VOCs observation site to the other two sites are approximately 4.6 km and 7.2 km, respectively.

In addition to ground-based measurements, hourly concentrations of ozone and NO_2 in August and September 2024 (wet season) and March 2025 (dry season) were collected from three automatic air quality monitoring stations located at ground level, 118 m, and 488 m on the Canton Tower *(Li et al., 2022b)*. The Canton Tower is situated in the Haizhu District, Guangzhou, approximately 12 km northwest of the VOCs observation site. In total, 21 and 7 ozone exceedance days were identified during the wet (August–September 2024) and dry (March 2025) seasons, respectively, forming the basis for the vertical transport quantification in subsequent analyses. To assess the spatial representativeness across these non-collocated sites, hourly O_3, NO_2, and Ox at GPMS and the Canton Tower surface level were compared during both seasons (Fig. S2). Hourly measurement of O_3, Ox, and NO_2 at the two sites all agreed well ($R^2 = 0.86$, 0.85, and 0.57; k = 0.84, 0.87, and 1.06). These vertical measurements span two intensive periods and are analyzed in Sections 3.3 and 3.4.

2.2 Box model simulation

A zero-dimension box model (F0AM) was used to quantify ozone and ROx radical budget and to assess ozone formation sensitivity at surface (Wolfe et al., 2016). The model employed the Master Chemical Mechanism (MCM) v3.3.1, coupled with an updated photolysis module of oxygenated VOCs (OVOCs) *(Peng et al., 2025)*. Model inputs included hourly observations of 59 VOCs at GPACS and of five trace gases (O_3, NO, NO_2, SO_2, and CO) at GPMS, together with three meteorological parameters (T, RH, and P), and photolysis rate coefficients (j-value). Missing observational data were gap-filled using linear interpolation. Eight key photolysis rates, namely $j(NO_2)$, $j(O^1D)$, $j(NO_3\text{-M})$, $j(NO_3\text{-R})$, $j(HCHO\text{-M})$, $j(HCHO\text{-R})$, $j(H_2O_2)$, $j(HONO)$, were calculated using the Tropospheric Ultraviolet and Visible (TUV) radiation model. Prior to each simulation, a 3-day model spin-up was performed to allow chemical species and radical

https://doi.org/10.5194/egusphere-2026-5887
Preprint. Discussion started: 9 November 2026
© Author(s) 2026. CC BY 4.0 License.

concentrations to reach steady state.

2.3 Column-integrated concentration (CIC) of trace gases

Based on vertically-resolved measurements of ozone and NO_2, the column-integrated concentration (CIC) within a defined air layer (e.g., the PBL and the nocturnal residual layer) was calculated following the method described by *Song et al. (2024)*, as formulated in Eq. 1.

$$CIC_{layer}(i)_t = \int_{h1}^{h2} [i]_h \frac{N_A}{V_{molar}(h)}\, dh \quad (1)$$

where $CIC_{layer}(i)_t$ is the CIC (*unit: molecules* cm^{-2}) of the species *i* within an air layer at time *t*. h_1 and h_2 (*unit: cm*) are the bottom and top height of the air layer, respectively. $[i]_h$ (*unit:* 10^{-9} *mol* mol^{-1}) is the volume mixing ratio of the species *i* at height *h*. N_A is Avogadro's constant (6.02×10^{23} mol^{-1}). $V_{molar}(h)$ (*unit:* cm^3 mol^{-1}) is the molar volume of gas at height *h*. Due to the height constraint of the Canton Tower, the vertical gradient measurements of air pollutants do not extend through the entire depth of the PBL. For the layer between the maximum measurement height and the top of the PBL or residual layer, pollutant concentrations were estimated using the interpolation method described by *Song et al. (2024)*.

2.4 Source apportionment of the daily ozone enhancement in PBL

As noted in previous studies *(Song et al., 2024; Li et al., 2022a)*, Ox (O_3+NO_2) serves as a more suitable metric for source apportionment of ozone within the PBL, as it reduces the influence of NO titration. Under typical daytime conditions, the enhancement of $CIC_{PBL}(Ox)$, denoted by $\Delta CIC_{PBL}(Ox)$, arises mainly from three contributing processes, namely the downward entrainment of ozone from the residual layer, net photochemical ozone production, and surface NO_2 emission. Entrainment and regional transport cannot be separated with the present observations, so the residual layer term in this study represents their net contribution. Details regarding the calculation methodology and its limitations are described in SI and follow the approach outlined in *Song et al. (2024)*. The PBL dataset was extracted from the ERA5 reanalysis hourly dataset published by the European Centre for Medium-Range Weather Forecasts

https://doi.org/10.5194/egusphere-2026-5887
Preprint. Discussion started: 9 November 2026
© Author(s) 2026. CC BY 4.0 License.

(ECMWF, https://cds.climate.copernicus.eu/datasets).

3. Results

3.1 Seasonal characteristics of ozone pollution in PRD

Over the past decade, surface ozone concentrations in the PRD have shown a persistent upward trend. This trend is illustrated using long-term ozone measurements from the Panyu Middle School monitoring station between 2013 and 2025 (Fig. 1a). Analysis reveals that the increase in ozone concentrations is primarily driven by changes in the dry season (October–March). From 2015 to 2025, surface ozone in the dry season increased at a statistically significant rate of 1.35 ppbv yr^{-1} ($p<0.01$). In contrast, wet season (April–September) concentrations showed a slight, statistically insignificant upward trend of 0.09 ppbv yr^{-1} ($p=0.64$). A similar seasonal contrast, namely the stronger ozone increases in the dry season and statistically insignificant trends in the wet season, was also evident at other urban sites in the PRD (Fig. S3a). The difference in surface ozone trends between the dry and wet seasons is closely linked to the long-term change in NOx concentrations over the same period. Compared with the wet season, NOx concentrations (represented here by NO_2) declined more sharply in the dry season, whereas Ox (O_3+NO_2) concentrations did not show a significant trend (Figs. 1b and S3b). This indicates a stronger weakening of the NO titration effect in the dry season, leading to a more pronounced upward trend in ozone (Li et al., 2022a). However, when evaluating ozone pollution against the Chinese National Ambient Air Quality Standard (defined as the days with a maximum daily average 8 h ozone concentration of greater than 81.6 ppbv), the number of exceedance days was greater in the wet season than in the dry season. This indicates that while most ozone exceedances currently occur during the wet season, the underlying upward trend in dry-season concentrations suggests that ozone pollution may become increasingly severe during this period in the future.

To examine the seasonal drivers of surface ozone pollution, measurements of ozone, its precursors (namely VOCs and NOx), and meteorological factors collected from July 1, 2024, to June 30, 2025 were analyzed. As shown in Fig. 2, distinct seasonal variations are evident in both meteorological conditions and air pollutant concentrations. In dry season, northerly winds prevailed, accompanied by lower temperature and RH.

https://doi.org/10.5194/egusphere-2026-5887
Preprint. Discussion started: 9 November 2026
© Author(s) 2026. CC BY 4.0 License.

In contrast, the wet season was characterized by southerly winds bringing warm and moist air masses. Except for isoprene, a typical tracer of biogenic emissions, the mean concentrations of other VOCs and air pollutants (NOx, CO, SO_2, $PM_{2.5}$, and PM_{10}) were substantially higher in the dry season than in the wet season (Fig. S4). Mean ozone concentrations were also slightly elevated in the dry season (35.4 ± 22.6 ppbv) compared to the wet season (32.2 ± 25.7 ppbv). Given the ongoing rising trend in dry-season ozone, the difference in mean ozone concentrations between the two seasons is likely to widen in the future.

3.2 Seasonal shift in photochemical ozone formation regime

Analysis of observed relationships among ozone, the OH reactivity of NOx (OHR_{NOx}), and the OH reactivity of VOCs (OHR_{VOCs}) indicates that ozone formation in the PRD is sensitive to both VOCs and NOx, primarily falling within the VOCs-limited and transition regimes (Fig. 3a). Box model simulations further clarify this seasonal distinction. The ozone formation sensitivity is predominantly within the VOCs-limited regime in the dry season but shifts toward the NOx-VOCs transition regime in the wet season (Fig. 3b). This shift highlights a fundamental difference in the driving chemical mechanisms of ozone formation between seasons.

On exceedance days (hereafter, the analysis mainly focused on the data of pollution days and will be not repeated), ozone formation is dominated by the HO_2+NO and RO_2+NO reaction pathways (Fig. 4a, 4c), with comparable fractional contributions in both seasons. However, the daytime mean ozone production rate, $P(O_3)$, in the wet season (25.5 ppbv h^{-1}) is approximately 3.4 times greater than in the dry season (7.4 ppbv h^{-1}). For ozone removal, the reaction NO_2+OH represents the primary sink, followed by ozone photolysis. The latter process proceeds 1.5 times faster in the wet season (0.71 ppbv h^{-1}) than in the dry season (0.47 ppbv h^{-1}). Consequently, the net ozone production rate, $P_{net}(O_3)$, in the wet season is 3.9 times that in the dry season, underscoring a more vigorous photochemical environment in the warmer months. This enhanced photochemical activity in the wet season is also reflected in the ROx radical budget. The primary formation pathway is $O(^1D)$+H_2O, while the dominant removal pathway is OH+NO_2. Both the formation and removal rates of ROx radicals are approximately 2.1 times higher in the wet season than in the dry season, consistent with the observed acceleration in ozone photochemistry.

https://doi.org/10.5194/egusphere-2026-5887
Preprint. Discussion started: 9 November 2026
© Author(s) 2026. CC BY 4.0 License.

In the wet season, mean temperatures are elevated compared to the dry season. Higher ambient temperatures promote the emissions of reactive biogenic VOCs (BVOCs), such as isoprene and monoterpenes, from vegetation. As shown in Fig. 5a, the total measured concentrations of VOCs were significantly higher in the dry season than in the wet season. However, the emission profile of anthropogenic VOCs showed little seasonal variation (Fig. S5). Notably, the mean concentration of isoprene increased substantially from 0.04 ppbv in the dry season to 0.25 ppbv in the wet season (Fig. S4). Consequently, while total VOCs concentrations peaked in the dry season, their total OH reactivity (OHR) is higher in the wet season. This seasonal pattern in VOCs is primarily characterized by enhanced anthropogenic emissions (reflected in elevated alkane concentrations) in the dry season and increased biogenic emissions (indicated by higher isoprene levels) in the wet season *(Zou et al., 2015)*.

Distinct diurnal patterns in VOCs concentrations and their OHRs were observed between seasons. In the dry season, both VOCs concentrations and OHRs showed similar diurnal profiles, with peaks occurring in the morning (around 10:00 LT) and at night (22:00–03:00 LT) (Fig. 5c–d). In contrast, the wet season exhibited a different pattern with VOCs concentrations peaked at night (around 00:00 LT, Fig. 5e), whereas the OHRs of VOCs displayed a pronounced daytime peak near noon (Fig. 5f). This midday OHR peak was driven significantly by enhanced isoprene levels. The increase in biogenic emissions in the wet season played a key role in elevating the total OHRs of VOCs (Fig. 3b). This shift helped drive the ozone formation regime toward a NOx-VOCs transition state and substantially increased the $P_{net}(O_3)$. Sensitivity analysis indicates that removing isoprene would reduce the mean daytime $P_{net}(O_3)$ by up to 21% (Fig. 4c). This highlights the important role of BVOCs in driving the enhanced photochemical ozone formation in the wet season, when elevated temperatures promote both increased BVOCs emissions and accelerated reaction rates. In addition, differences in radiation, PBL dynamics, and other VOCs may also contribute to the seasonal contrast.

3.3 Relative importance of chemical formation and vertical transport

As shown in Fig. 6a, the average levels and diurnal patterns of surface ozone and solar radiation on exceedance days were broadly similar between the dry and wet seasons. Given that the photochemical ozone production is significantly stronger in the

https://doi.org/10.5194/egusphere-2026-5887
Preprint. Discussion started: 9 November 2026
© Author(s) 2026. CC BY 4.0 License.

wet season, other factors must be responsible for the rapid rise in surface ozone observed after sunrise in the dry season.

Time series of surface $P_{net}(O_3)$ and ozone concentrations at three altitudes on the Canton Tower, from representative episodes in each season, are shown in Fig. S6. Ozone concentrations generally increased with height in both seasons, but nocturnal vertical gradients were substantially stronger in the dry season. These positive vertical ozone gradients, particularly at night, are primarily attributed to the inhomogeneous vertical distribution of NO and its titration effect *(Li et al., 2025)*. Thus, the stronger vertical ozone gradients in the dry season were likely a combined result of enhanced NOx emissions and greater atmospheric stability *(Song et al., 2024)*.

Notable differences in diurnal ozone variability were also observed aloft. In the wet season, the ozone concentrations at both the surface and 488 m all increased rapidly after sunrise, showing clear diurnal cycles. In contrast, ozone at 488 m exhibited much weaker diurnal variation compared to the surface in the dry season. The combination of higher concentrations and dampened diurnal variability aloft suggests that the downward transport of ozone, driven by daytime PBL expansion, plays a key role in causing the rapid post-sunrise increase in surface ozone during the dry season *(Li et al., 2018)*.

To account for the influence of NO titration, we used Ox as a more robust metric for analyzing vertical and diurnal ozone variations. As shown in Fig.6 b-c, the daily enhancements of Ox (defined as the difference of Ox concentrations between 16:00 LT and 08:00 LT) at 488 m in the wet season were moderately higher than those at the surface. Similar to surface observations, Ox concentrations at 488 m rose rapidly after sunrise, independent of the PBL evolution. Furthermore, daily maximum surface ozone concentrations correlated reasonably well with daily maximum $P_{net}(O_3)$ values (k=0.48, R^2=0.36, Fig. S7). These results indicate that enhanced photochemical formation was an importan driver of the rapid ozone increase throughout the entire PBL in the wet season.

In the dry season, daily maximum surface ozone concentrations showed a weak dependence on $P_{net}(O_3)$ (k=1.44, R^2=0.24, Fig. S7). In addition, daily enhancements of Ox at 488 m were also significantly lower than those at the surface. The onset of the Ox increase at 488 m was delayed by approximately three hours relative to the surface (Fig.

https://doi.org/10.5194/egusphere-2026-5887
Preprint. Discussion started: 9 November 2026
© Author(s) 2026. CC BY 4.0 License.

6b), coinciding with the time when the growing PBL reached this altitude (Fig. 6c). Together, these findings demonstrate that photochemical ozone production was weak throughout the PBL in the dry season, and that the morning rise in surface ozone was largely driven by the downward transport of ozone-rich air from aloft as the PBL developed.

The average column-integrated concentrations (CICs) of ozone in the PBL, denoted by $CIC_{PBL}(O_3)$, were significantly higher in the dry season than in the wet season, both in the morning (before 10:00 LT) and afternoon (after 13:00 LT; Fig. 6d). The average PBL heights (PBLHs) between 13:00 and 17:00 LT in the dry season were nearly 1.5 times greater than in the wet season, primarily explaining the larger daytime $CIC_{PBL}(O_3)$. Notably, the seasonal contrast in $CIC_{PBL}(O_3)$ was most pronounced at night, even though nocturnal PBLH differed only minimally. Quantitatively, $CIC_{PBL}(O_3)$ increased by more than 360% from 08:00 to 16:00 LT in the wet season, compared to only about 170% in the dry season (Fig. 6f). Similarly, the overnight decrease in $CIC_{PBL}(O_3)$ (from 16:00 to 08:00 LT the following day) exceeded 70% in the wet season but was only approximately 57% in the dry season. These patterns indicate that, in addition to weaker photochemical ozone production, the nocturnal removal of ozone within the PBL was also less efficient in the dry season. Consequently, the differing diurnal variation in $CIC_{PBL}(O_3)$ highlights the distinct fate of ozone between the two seasons during the observed episodes.

A deeper PBL provides a larger reservoir for ozone aloft. As the PBL expands rapidly during the day, this stored ozone can be recirculated downward, driving the rapid rise in surface concentrations. The coupled diurnal variation of PBLH and surface ozone supports this mechanism. In the wet season, mean surface ozone and PBLH increased at nearly the same rate, both peaking around 14:00 LT. In the dry season, the daily peaks of both surface ozone and PBLH were delayed by approximately three hours compared to the wet season. In contrast, the timing of the daily peaks in ambient temperature (Fig. S8) and solar radiation (Fig. 6a) showed no significant seasonal shift. This decoupling from photochemical drivers further confirms that the downward transport of ozone from aloft is a key factor in the formation of surface ozone pollution in the dry season.

3.4 Source apportionment of daytime ozone enhancement

https://doi.org/10.5194/egusphere-2026-5887
Preprint. Discussion started: 9 November 2026
© Author(s) 2026. CC BY 4.0 License.

Ozone retained aloft at night, primarily within the nocturnal residual layer, can be recirculated downward to the surface during daytime PBL expansion, contributing to the rapid rise in surface ozone. This physical transport process is closely coupled with local photochemical ozone production. To quantitatively assess the roles of vertical transport and photochemical formation in driving surface ozone pollution, the enhancement of PBL-integrated Ox, denoted as $\Delta CIC_{PBL}(Ox)$, was apportioned based on the changes in $CIC_{PBL}(Ox)$ and $CIC_{PBL}(NOx)$ (Song et al., 2024). Contributions of three sources, namely residual layer contribution, chemical formation, and surface emission (referring to the fraction of primarily-emitted NO_2 in Ox), were quantified using this method.

As shown in Fig. 7, $\Delta CIC_{PBL}(Ox)$ rapidly increased after sunrise, concurrent with PBL expansion. In the dry season, the downward transport of ozone from the residual layer was the dominant driver of the morning increase in $\Delta CIC_{PBL}(Ox)$ (Fig. 7a), a contribution that also includes ozone advected into the region. Its contribution rose sharply from 58% at 08:00 LT to 91% by 11:00 LT (Fig. 7b), coinciding with the period of most rapid PBL growth (Fig. 6e). This contribution subsequently declined to 68% in the afternoon as photochemical production increased. Overall, photochemical production contributed only a minor fraction (3%–31%) to $\Delta CIC_{PBL}(Ox)$ in the dry season. In contrast, the wet season was characterized by a stronger photochemical contribution. Between 08:00 and 14:00 LT, photochemical formation accounted for an average of 53% of $\Delta CIC_{PBL}(Ox)$, significantly higher than the contribution from the residual layer (45%). This apportionment result is consistent with the box-model simulations and further highlights the fundamental difference in the dominant drivers of surface ozone pollution between the wet (photochemically driven) and dry (dynamically driven) seasons in the PRD.

4. Conclusions

The PRD region, influenced by a distinct monsoon climate, serves as a typical case where the key drivers of surface ozone pollution vary markedly between wet and dry seasons. In the wet season, reactive biogenic VOCs (BVOCs) released from vegetation play an important role in contributing to the exceedance of surface ozone. With ongoing efforts to increase green cover and restore ecosystems, the emissions of BVOCs are projected to rise in the future. In this context, more stringent and effective reductions in

https://doi.org/10.5194/egusphere-2026-5887
Preprint. Discussion started: 9 November 2026
© Author(s) 2026. CC BY 4.0 License.

anthropogenic emissions of VOCs will be essential to offset the ozone formation potential from natural sources.

In contrast, the observed dry-season period is characterized by the dominant influence of vertical ozone recirculation within the PBL. The middle and upper sections of a well-developed PBL can act as a reservoir for ozone, which is then transported downward to the surface during daytime PBL expansion. It should be noted that ozone stored aloft may originate from both local photochemical production and regional transport, though the current analysis suggests local production is a significant contributor. In the dry season, both ozone production and removal processes are generally subdued, allowing ozone to accumulate aloft through persistent downward entrainment. This gradually builds up ozone concentrations near the surface, leading to the occurrence of pollution episodes near the surface. Consequently, short-term emergency emission controls may have limited effectiveness in mitigating ozone pollution in the dry season, as they do not substantially reduce the ozone already stored aloft. This suggests that proactively reducing precursor emissions before conditions are expected to stabilize may help reduce the accumulation of ozone in the upper atmosphere, thereby enhancing the overall effectiveness of ozone pollution mitigation strategies. Longer and more continuous vertical observations may be needed to determine whether these mechanisms operate throughout the monsoon cycle.

Data availability

The datasets used and/or analyzed during the current study available from the corresponding author on reasonable request.

Author contributions

YZ and XBL conceived the research. ZL and XS performed the data analysis, with contributions from YZ, XBL, and BY. ZL and XBL prepared the manuscript with contributions from YZ, XS, BY, CP, YP, JC, XW, and MS. All the authors reviewed the manuscript.

Competing interests

At least one of the (co-)authors is a member of the editorial board of Atmospheric

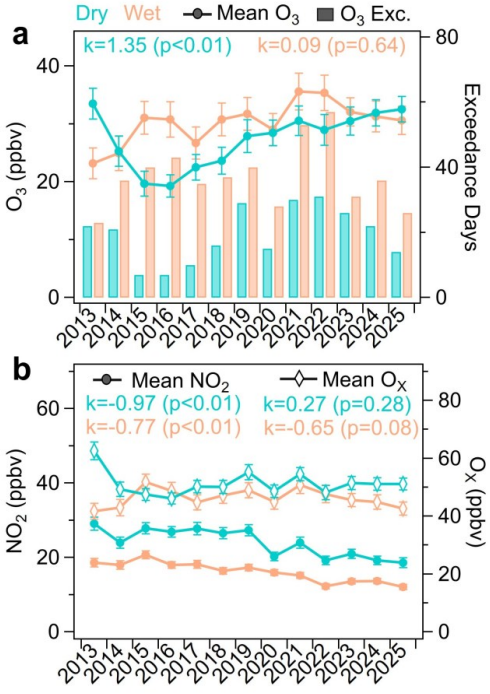
https://doi.org/10.5194/egusphere-2026-5887
Preprint. Discussion started: 9 November 2026
© Author(s) 2026. CC BY 4.0 License.

Chemistry and Physics.

Acknowledgment

This work was financially supported by the National Key R&D Plan of China (grant no. 2023YFC3710900), the National Natural Science Foundation of China (grant no. 42577124, 42305095, and 42475107), Guangdong Basic and Applied Basic Research Foundation (grant no. 2026A1515010897 and 2024A1515011570), the Key Innovation Team of Guangdong Meteorological Bureau (grant no. GRMCTD202506-ZD06), Guangdong Province: Special Support Plan for High-Level Talents (grant no. 2023JC07L057), and Guangdong Provincial General Colleges and Universities Innovation Team Project (Natural Science) (grant no. 2024KCXTD004), and the Excellent Graduate Student Cultivation Program of Jinan University (grant no. 2026CXB077).

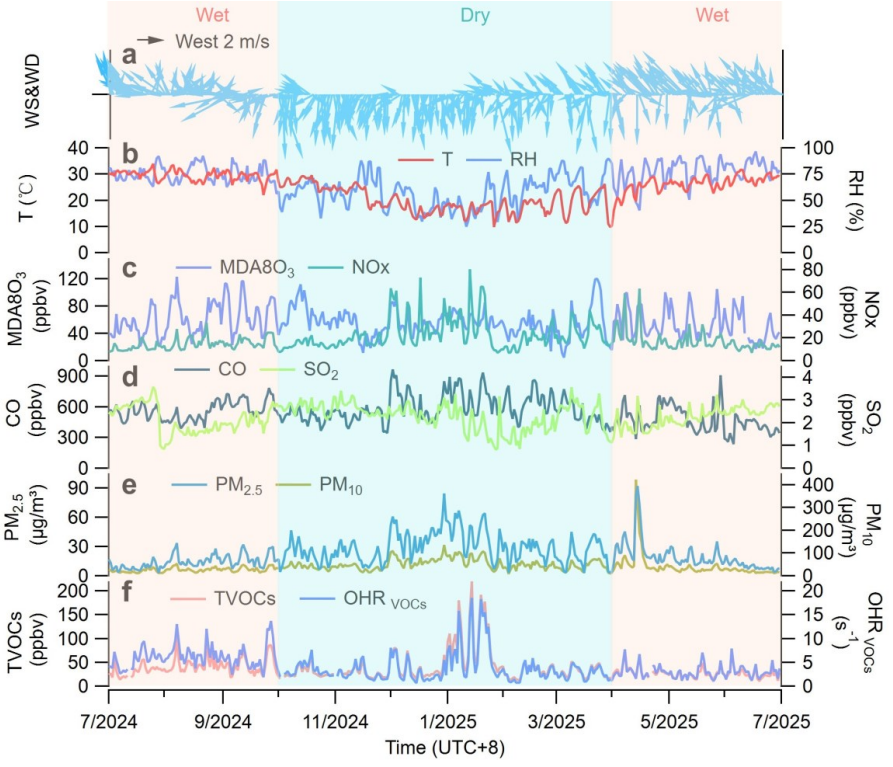
https://doi.org/10.5194/egusphere-2026-5887
Preprint. Discussion started: 9 November 2026
© Author(s) 2026. CC BY 4.0 License.



406

407 **Fig. 1 Seasonal characteristics of ozone pollution in the PRD. a,** Interannual
408 variation in ozone exceedance days and mean surface concentration at the Guangzhou
409 Panyu Middle School site. **b,** Interannual variation in mean surface concentrations of
410 NO_2 and Ox at the Guangzhou Panyu Middle School site. Error bars represent s.d.
411 (scaled to 10% for display clarity). The *k* values indicate the long-term trends of surface
412 ozone over the period of 2015-2025.

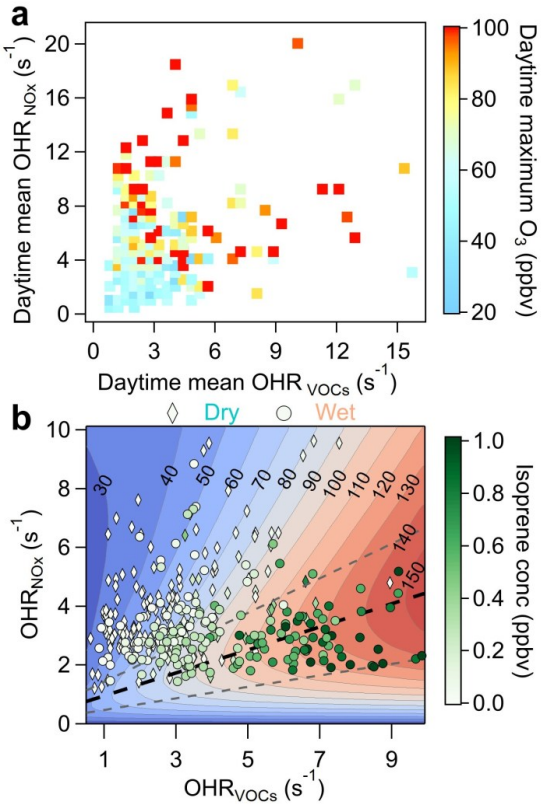
https://doi.org/10.5194/egusphere-2026-5887
Preprint. Discussion started: 9 November 2026
© Author(s) 2026. CC BY 4.0 License.



413

414 **Fig. 2 Time series of meteorological factors and concentrations of air pollutants**
415 **during the campaign. a,** Wind speed and wind direction. **b,** Temperature and relative
416 humidity. **c,** Daily maximum 8-hour average O_3 and NOx. **d,** CO and SO_2. **e,** $PM_{2.5}$ and
417 PM_{10}. **f,** Total VOCs concentration and its OHRs.

https://doi.org/10.5194/egusphere-2026-5887
Preprint. Discussion started: 9 November 2026
© Author(s) 2026. CC BY 4.0 License.



418

419 **Fig. 3 Daily maximum ozone concentration and OHR relationship chart for its**
420 **precursors. a,** Observational scatter plot of daytime (6:00-18:00 LT) means OHR_{VOCs}
421 versus daytime mean OHR_{NOx}. Colors of the squares represent the daily maximum
422 ozone concentrations. **b,** The model-based isopleth diagram of daily maximum ozone
423 against the reactivity of NOx (OHR_{NOx}) and VOCs (OHR_{VOCs}). The circles indicate the
424 daytime mean values of OHR_{NOx} and OHR_{VOCs} in wet season. The diamonds indicate
425 the daytime mean values of OHR_{NOx} and VOCs OHR_{VOCs} in dry season. Colors of the
426 circles and diamonds represent the daytime mean isoprene concentration.

https://doi.org/10.5194/egusphere-2026-5887
Preprint. Discussion started: 9 November 2026
© Author(s) 2026. CC BY 4.0 License.

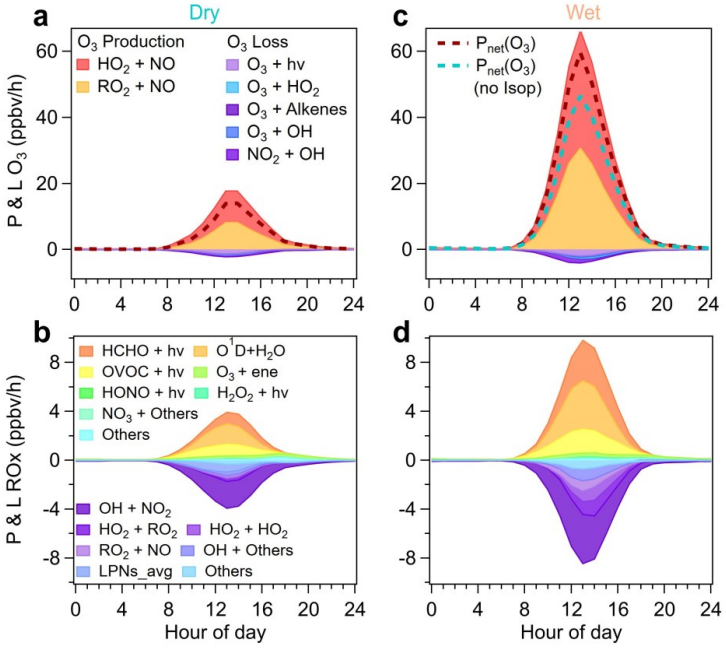


Fig. 4 Average diurnal variation and contribution pathways of ozone and ROx radical budgets on ozone exceedance days in the dry (**a, b**) and wet (**c, d**) season.

https://doi.org/10.5194/egusphere-2026-5887
Preprint. Discussion started: 9 November 2026
© Author(s) 2026. CC BY 4.0 License.

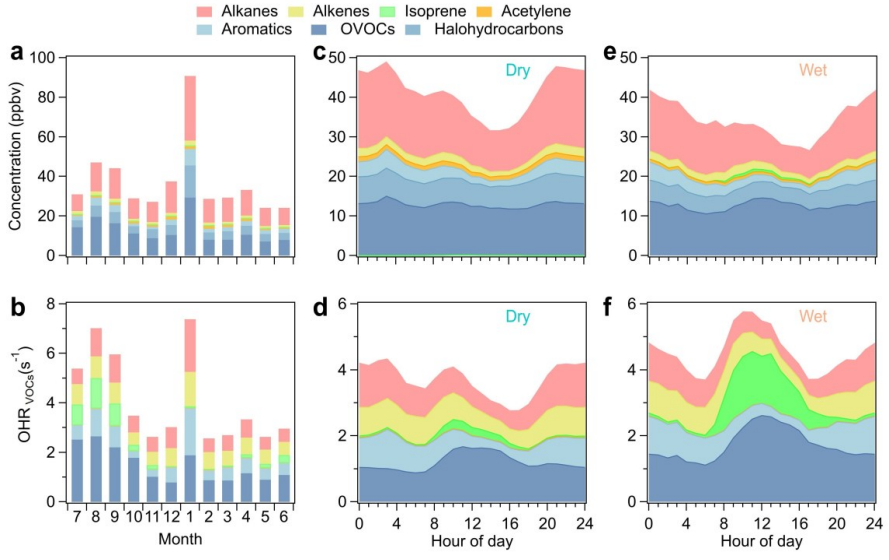


Fig. 5 Temporal variation in concentration and OHR of VOCs. a, b, Seasonal variation in monthly mean concentration and OHR of different VOC groups. **c, d,** Average diurnal variation in concentration and OHR of different VOC groups in the dry season. **e, f,** Average diurnal variation in concentration and OHR of different VOC groups in the wet season.

https://doi.org/10.5194/egusphere-2026-5887
Preprint. Discussion started: 9 November 2026
© Author(s) 2026. CC BY 4.0 License.

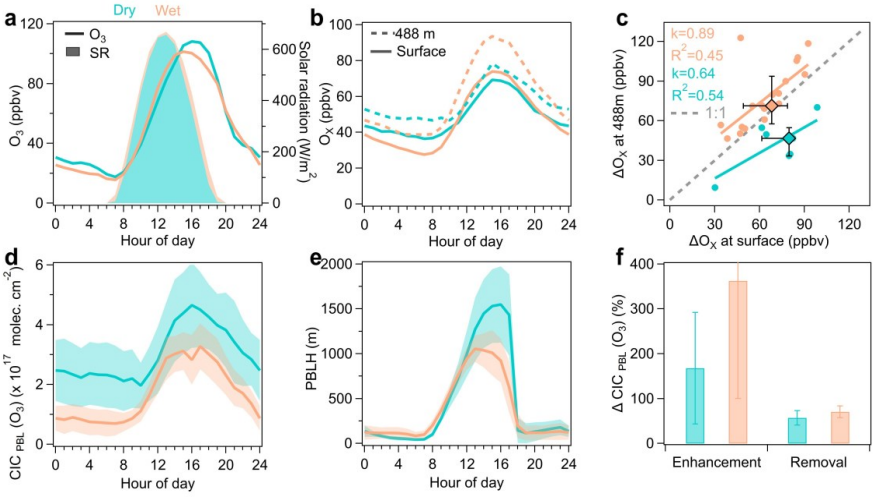
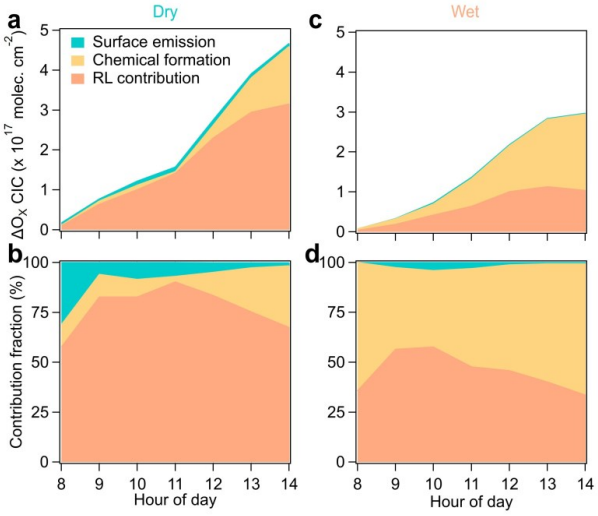


Fig. 6 Daily ozone enhancement on exceedance days in the wet and dry seasons. a, Average diurnal variation in surface ozone concentrations and solar radiation (SR) at the Guangzhou Panyu Middle School site. **b,** Average diurnal variation in Ox (O_3+NO_2) concentrations at the surface and 488 m at the Canton tower site. **c,** Scatter plots of daily Ox enhancement (ΔOx) at 488 m versus those at the surface. The diamonds represent median values and error bars show the 25–75th percentiles. The solid lines represent linear fittings with showing their slopes (*k*) and coefficients of determination (R^2). **d,** Average diurnal variation in $CIC_{PBL}(O_3)$. Error bars show ±s.d. **e,** Average diurnal variation in PBLH. Error bars show ±s.d. **f,** The relative change in average daily enhancement and removal of $CIC_{PBL}(O_3)$. Error bars show ±s.d.

https://doi.org/10.5194/egusphere-2026-5887
Preprint. Discussion started: 9 November 2026
© Author(s) 2026. CC BY 4.0 License.



447

448 **Fig. 7 Source contributions to the ΔCIC$_{PBL}$(Ox) on exceedance days in the wet and**
449 **dry seasons. a, b,** Average diurnal variations in the absolute and fractional
450 contributions of the three sources to ΔCIC$_{PBL}$(Ox) in the dry season. **c, d,** Average
451 diurnal variations in absolute and fractional contributions of the three sources to
452 ΔCIC$_{PBL}$(Ox) in the wet season.

https://doi.org/10.5194/egusphere-2026-5887
Preprint. Discussion started: 9 November 2026
© Author(s) 2026. CC BY 4.0 License.

References

Agathokleous, E., Feng, Z., and Sicard, P.: Surge in nocturnal ozone pollution, Science, 382, 1131-1131, doi:10.1126/science.adm7628, 2023.

Canaval, E., Millet, D. B., Zimmer, I., Nosenko, T., Georgii, E., Partoll, E. M., Fischer, L., Alwe, H. D., Kulmala, M., Karl, T., Schnitzler, J.-P., and Hansel, A.: Rapid conversion of isoprene photooxidation products in terrestrial plants, Communications Earth & Environment, 1, 44, 10.1038/s43247-020-00041-2, 2020.

Cao, J., Situ, S., Hao, Y., Xie, S., and Li, L.: Enhanced summertime ozone and SOA from biogenic volatile organic compound (BVOC) emissions due to vegetation biomass variability during 1981–2018 in China, Atmos. Chem. Phys., 22, 2351-2364, 10.5194/acp-22-2351-2022, 2022.

Cheng, N., Chen, Z., Sun, F., Sun, R., Dong, X., Xie, X., and Xu, C.: Ground ozone concentrations over Beijing from 2004 to 2015: Variation patterns, indicative precursors and effects of emission-reduction, Environ Pollut, 237, 262-274, https://doi.org/10.1016/j.envpol.2018.02.051, 2018.

Ding, A. J., Wang, T., Thouret, V., Cammas, J. P., and Nédélec, P.: Tropospheric ozone climatology over Beijing: analysis of aircraft data from the MOZAIC program, Atmos. Chem. Phys., 8, 1-13, 10.5194/acp-8-1-2008, 2008.

He, H., Liang, X. Z., Sun, C., Tao, Z., and Tong, D. Q.: The long-term trend and production sensitivity change in the US ozone pollution from observations and model simulations, Atmos. Chem. Phys., 20, 3191-3208, 10.5194/acp-20-3191-2020, 2020.

He, Y. J., Uno, I., Wang, Z. F., Pochanart, P., Li, J., and Akimoto, H.: Significant impact of the East Asia monsoon on ozone seasonal behavior in the boundary layer of Eastern China and the west Pacific region, Atmos. Chem. Phys., 8, 7543-7555, 10.5194/acp-8-7543-2008, 2008.

Huang, J.-P., Fung, J. C. H., and Lau, A. K. H.: Integrated processes analysis and systematic meteorological classification of ozone episodes in Hong Kong, J. Geophys. Res. Atmos., 111, https://doi.org/10.1029/2005JD007012, 2006.

Huang, J.-P., Fung, J. C. H., Lau, A. K. H., and Qin, Y.: Numerical simulation and process analysis of typhoon-related ozone episodes in Hong Kong, J. Geophys. Res. Atmos., 110, https://doi.org/10.1029/2004JD004914, 2005.

Klein, A., Ravetta, F., Thomas, J. L., Ancellet, G., Augustin, P., Wilson, R., Dieudonné, E., Fourmentin, M., Delbarre, H., and Pelon, J.: Influence of vertical mixing and nighttime transport on surface ozone variability in the morning in Paris and the surrounding region, Atmos Environ, 197, 92-102, https://doi.org/10.1016/j.atmosenv.2018.10.009, 2019.

Li, K., Jacob, D. J., Liao, H., Qiu, Y., Shen, L., Zhai, S., Bates, K. H., Sulprizio, M. P., Song, S., Lu, X., Zhang, Q., Zheng, B., Zhang, Y., Zhang, J., Lee, H. C., and Kuk, S. K.: Ozone pollution in the North China Plain spreading into the late-winter haze season, PNAS, 118, e2015797118, doi:10.1073/pnas.2015797118, 2021a.

Li, X.-B., Wang, D.-S., Lu, Q.-C., Peng, Z.-R., and Wang, Z.-Y.: Investigating vertical distribution patterns of lower tropospheric PM2.5 using unmanned aerial vehicle

https://doi.org/10.5194/egusphere-2026-5887
Preprint. Discussion started: 9 November 2026
© Author(s) 2026. CC BY 4.0 License.

measurements, Atmos Environ, 173, 62-71, https://doi.org/10.1016/j.atmosenv.2017.11.009, 2018.

Li, X.-B., Fan, G., Lou, S., Yuan, B., Wang, X., and Shao, M.: Transport and boundary layer interaction contribution to extremely high surface ozone levels in eastern China, Environ Pollut, 268, 115804, https://doi.org/10.1016/j.envpol.2020.115804, 2021b.

Li, X.-B., Wang, D.-S., Lu, Q.-C., Peng, Z.-R., Lu, S.-J., Li, B., and Li, C.: Three-dimensional investigation of ozone pollution in the lower troposphere using an unmanned aerial vehicle platform, Environ Pollut, 224, 107-116, https://doi.org/10.1016/j.envpol.2017.01.064, 2017.

Li, X.-B., Yuan, B., Parrish, D. D., Chen, D., Song, Y., Yang, S., Liu, Z., and Shao, M.: Long-term trend of ozone in southern China reveals future mitigation strategy for air pollution, Atmos Environ, 269, 10.1016/j.atmosenv.2021.118869, 2022a.

Li, X.-B., Yuan, B., Wang, S., Wang, C., Lan, J., Liu, Z., Song, Y., He, X., Huangfu, Y., Pei, C., Cheng, P., Yang, S., Qi, J., Wu, C., Huang, S., You, Y., Chang, M., Zheng, H., Yang, W., Wang, X., and Shao, M.: Variations and sources of volatile organic compounds (VOCs) in urban region: insights from measurements on a tall tower, Atmos. Chem. Phys., 22, 10567-10587, 10.5194/acp-22-10567-2022, 2022b.

Li, X., Wang, W., Yang, S., Cheng, Y., Zeng, L., Yu, X., Lu, S., Liu, Y., Hu, M., Xie, S., Huang, X., Zhou, J., Shi, L., Xu, H., Lin, S., Liu, H., Feng, M., Song, D., Tan, Q., and Zhang, Y.: Ozone sensitivity regimes vary at different heights in the planetary boundary layer, Sci Total Environ, 944, 173712, https://doi.org/10.1016/j.scitotenv.2024.173712, 2024.

Li, X. B., Yuan, B., Huangfu, Y., Yang, S., Song, X., Qi, J., He, X., Wang, S., Chen, Y., Yang, Q., Song, Y., Peng, Y., Tang, G., Gao, J., Gu, D., and Shao, M.: Vertical changes in volatile organic compounds (VOCs) and impacts on photochemical ozone formation, Atmos. Chem. Phys., 25, 2459-2472, 10.5194/acp-25-2459-2025, 2025.

Li, Y., Lau, A. K.-H., Fung, J. C.-H., Zheng, J. Y., Zhong, L. J., and Louie, P. K. K.: Ozone source apportionment (OSAT) to differentiate local regional and super-regional source contributions in the Pearl River Delta region, China, J. Geophys. Res. Atmos., 117, https://doi.org/10.1029/2011JD017340, 2012.

Lu, H., Zeng, J., Song, W., Pei, C., Zhang, J., Tian, X., Tang, W., Fang, L., Zhang, Y., Geng, L., and Wang, X.: Typhoon Subsidence Intensity Flips Surface Ozone Spikes From Photochemical Production to Vertical Transport, 131, e2025JD044948, https://doi.org/10.1029/2025JD044948, 2026.

Ma, W., Xing, C., Wang, W., Zhang, Q., Wang, Z., Yang, Y., and Liu, C.: Ozone pollution monitoring using a full-time hyperspectral tomography system for multiple air pollutants, Nature Communications, 17, 245, 10.1038/s41467-025-66944-w, 2025.

Mathur, R., Hogrefe, C., Hakami, A., Zhao, S., Szykman, J., and Hagler, G.: A Call for an Aloft Air Quality Monitoring Network: Need, Feasibility, and Potential Value, Environ Sci Technol, 52, 10903-10908, 10.1021/acs.est.8b02496, 2018.

Peng, Y., Yuan, B., Wang, S., Song, X., Peng, Z., Wang, W., Yang, S., Qi, J., He, X., Huangfu, Y., Li, X. B., and Shao, M.: A new parameterization of photolysis rates for oxygenated volatile organic compounds (OVOCs), Atmos. Chem. Phys., 25, 7037-

https://doi.org/10.5194/egusphere-2026-5887
Preprint. Discussion started: 9 November 2026
© Author(s) 2026. CC BY 4.0 License.



7052, 10.5194/acp-25-7037-2025, 2025.

Perdigones, B. C., Lee, S., Cohen, R. C., Park, J.-H., and Min, K.-E.: Two Decades of Changes in Summertime Ozone Production in California's South Coast Air Basin, Environ Sci Technol, 56, 10586-10595, 10.1021/acs.est.2c01026, 2022.

Pfannerstill, E. Y., Arata, C., Zhu, Q., Schulze, B. C., Ward, R., Woods, R., Harkins, C., Schwantes, R. H., Seinfeld, J. H., Bucholtz, A., Cohen, R. C., and Goldstein, A. H.: Temperature-dependent emissions dominate aerosol and ozone formation in Los Angeles, Science, 384, 1324-1329, doi:10.1126/science.adg8204, 2024.

Qin, M., She, Y., Wang, M., Wang, H., Chang, Y., Tan, Z., An, J., Huang, J., Yuan, Z., Lu, J., Wang, Q., Liu, C., Liu, Z., Xie, X., Li, J., Liao, H., Pye, H. O. T., Huang, C., Guo, S., Hu, M., Zhang, Y., Jacob, D. J., and Hu, J.: Increased urban ozone in heatwaves due to temperature-induced emissions of anthropogenic volatile organic compounds, Nat. Geosci., 18, 50-56, 10.1038/s41561-024-01608-w, 2025.

Shao, M., Wang, W., Yuan, B., Parrish, D. D., Li, X., Lu, K., Wu, L., Wang, X., Mo, Z., Yang, S., Peng, Y., Kuang, Y., Chen, W., Hu, M., Zeng, L., Su, H., Cheng, Y., Zheng, J., and Zhang, Y.: Quantifying the role of PM2.5 dropping in variations of ground-level ozone: Inter-comparison between Beijing and Los Angeles, Sci Total Environ, 788, 10.1016/j.scitotenv.2021.147712, 2021.

Song, X., Li, X.-B., Yuan, B., He, X., Chen, Y., Wang, S., Huangfu, Y., Peng, Y., Zhang, C., Liu, A., Yang, H., Liu, C., Li, J., and Shao, M.: Elucidating key factors in regulating budgets of ozone and its precursors in atmospheric boundary layer, npj Climate and Atmospheric Science, 7, 262, 10.1038/s41612-024-00818-8, 2024.

Song, Y., Liu, C., Li, X.-B., Yuan, B., Wang, S., Yang, S., Peng, Y., Chang, M., Wang, X., and Shao, M.: Characteristics of Volatile Organic Compounds in Megacity Shenzhen, China: Seasonal Variation, Temperature Dependence, and Source Apportionment, ACS Earth and Space Chemistry, 9, 1825-1836, 10.1021/acsearthspacechem.5c00082, 2025.

Udina, M., Soler, M. R., Olid, M., Jiménez-Esteve, B., and Bech, J.: Pollutant vertical mixing in the nocturnal boundary layer enhanced by density currents and low-level jets: two representative case studies, Boundary-Layer Meteorology, 174, 203-230, 10.1007/s10546-019-00483-y, 2020.

Wang, H., Ma, X., Tan, Z., Wang, H., Chen, X., Chen, S., Gao, Y., Liu, Y., Liu, Y., Yang, X., Yuan, B., Zeng, L., Huang, C., Lu, K., and Zhang, Y.: Anthropogenic monoterpenes aggravating ozone pollution, National Science Review, 9, 10.1093/nsr/nwac103, 2022a.

Wang, N., Huang, X., Xu, J., Wang, T., Tan, Z.-m., and Ding, A.: Typhoon-boosted biogenic emission aggravates cross-regional ozone pollution in China, Sci. Adv., 8, eabl6166, doi:10.1126/sciadv.abl6166, 2022b.

Wang, T., Xue, L., Brimblecombe, P., Lam, Y. F., Li, L., and Zhang, L.: Ozone pollution in China: A review of concentrations, meteorological influences, chemical precursors, and effects, Sci Total Environ, 575, 1582-1596, https://doi.org/10.1016/j.scitotenv.2016.10.081, 2017.

Wang, Z., Zhang, H., Shi, C., Ji, X., Zhu, Y., Xia, C., Sun, X., Zhang, M., Lin, X., Yan, S., Zhou, Y., Xing, C., Chen, Y., and Liu, C.: Vertical and spatial differences in ozone

https://doi.org/10.5194/egusphere-2026-5887
Preprint. Discussion started: 9 November 2026
© Author(s) 2026. CC BY 4.0 License.

formation sensitivities under different ozone pollution levels in eastern Chinese cities, npj Climate and Atmospheric Science, 8, 30, 10.1038/s41612-024-00855-3, 2025.

Wolfe, G. M., Marvin, M. R., Roberts, S. J., Travis, K. R., and Liao, J.: The Framework for 0-D Atmospheric Modeling (F0AM) v3.1, Geosci. Model Dev., 9, 3309-3319, 10.5194/gmd-9-3309-2016, 2016.

Wu, Y., Chen, W., You, Y., Xie, Q., Jia, S., and Wang, X.: Quantitative impacts of vertical transport on the long-term trend of nocturnal ozone increase over the Pearl River Delta region during 2006–2019, Atmos. Chem. Phys., 23, 453-469, 10.5194/acp-23-453-2023, 2023.

Xing, C., Liu, C., Ye, C., Xue, J., Wu, H., Ji, X., Ou, J., and Hu, Q.: Observations of the vertical distributions of summertime atmospheric pollutants in Nam Co: OH production and source analysis, Atmos. Chem. Phys., 24, 10093-10112, 10.5194/acp-24-10093-2024, 2024.

Yang, L., Yuan, Z., Luo, H., Wang, Y., Xu, Y., Duan, Y., and Fu, Q.: Identification of long-term evolution of ozone sensitivity to precursors based on two-dimensional mutual verification, Sci Total Environ, 760, 143401, https://doi.org/10.1016/j.scitotenv.2020.143401, 2021.

Yates, E. L., Iraci, L. T., Austerberry, D., Pierce, R. B., Roby, M. C., Tadić, J. M., Loewenstein, M., and Gore, W.: Characterizing the impacts of vertical transport and photochemical ozone production on an exceedance area, Atmos Environ, 109, 342-350, https://doi.org/10.1016/j.atmosenv.2014.09.002, 2015.

Zeng, J., Zhang, Y., Mu, Z., Pang, W., Zhang, H., Wu, Z., Song, W., and Wang, X.: Temperature and light dependency of isoprene and monoterpene emissions from tropical and subtropical trees: Field observations in south China, Applied Geochemistry, 155, 105727, https://doi.org/10.1016/j.apgeochem.2023.105727, 2023.

Zhang, Y., Yu, S., Chen, X., Li, Z., Li, M., Song, Z., Liu, W., Li, P., Zhang, X., Lichtfouse, E., and Rosenfeld, D.: Local production, downward and regional transport aggravated surface ozone pollution during the historical orange-alert large-scale ozone episode in eastern China, Environ. Chem. Lett., 20, 1577-1588, 10.1007/s10311-022-01421-0, 2022.

Zhao, M., Zhang, Y., Pei, C., Chen, T., Mu, J., Liu, Y., Wang, Y., Wang, W., and Xue, L.: Worsening ozone air pollution with reduced NOx and VOCs in the Pearl River Delta region in autumn 2019: Implications for national control policy in China, Journal of Environmental Management, 324, 116327, https://doi.org/10.1016/j.jenvman.2022.116327, 2022.

Zhou, X., Li, M., Huang, X., Liu, T., Zhang, H., Qi, X., Wang, Z., Qin, Y., Geng, G., Wang, J., Chi, X., and Ding, A.: Urban meteorology–chemistry coupling in compound heat–ozone extremes, Nature Cities, 2, 847-856, 10.1038/s44284-025-00302-1, 2025.

Zou, Y., Guan, X. H., Flores, R. M., Yan, X. L., Fan, L. Y., Deng, T., Deng, X. J., and Ye, D. Q.: Revealing the Influencing Factors of an Oxygenated Volatile Organic Compounds (OVOCs) Source Apportionment Model: A Case Study of a Dense Urban Agglomeration in the Winter, J. Geophys. Res. Atmos., 129, e2023JD039401,

https://doi.org/10.5194/egusphere-2026-5887
Preprint. Discussion started: 9 November 2026
© Author(s) 2026. CC BY 4.0 License.



https://doi.org/10.1029/2023JD039401, 2024.

Zou, Y., Guan, X. H., Flores, R. M., Yan, X. L., Liang, X. J., Fan, L. Y., Deng, T., Deng, X. J., Ye, D. Q., and Doskey, P. V.: Optimizing Source Apportionment of OVOCs With Machine Learning-Enhanced Photochemical Models, 130, e2024JD043080, https://doi.org/10.1029/2024JD043080, 2025.

Zou, Y., Deng, X. J., Zhu, D., Gong, D. C., Wang, H., Li, F., Tan, H. B., Deng, T., Mai, B. R., Liu, X. T., and Wang, B. G.: Characteristics of 1 year of observational data of VOCs, NOx and O3 at a suburban site in Guangzhou, China, Atmos. Chem. Phys., 15, 6625-6636, 10.5194/acp-15-6625-2015, 2015.